Journal Pre-proof

Mechanisms of broad-band ultraviolet B irradiation-induced itch in mice

Liang Cao, Xueping Yue, Yonghui Zhao, Lixia Du, Zili Xie, Yi Yuan, Sha Zhang, Feng Li, Jing Feng, Hongzhen Hu

PII: S0022-202X(21)01129-5

DOI: https://doi.org/10.1016/j.jid.2021.03.015

Reference: JID 2885

To appear in: *The Journal of Investigative Dermatology*

Received Date: 9 November 2020

Revised Date: 2 March 2021

Accepted Date: 9 March 2021

Please cite this article as: Cao L, Yue X, Zhao Y, Du L, Xie Z, Yuan Y, Zhang S, Li F, Feng J, Hu H, Mechanisms of broad-band ultraviolet B irradiation-induced itch in mice, *The Journal of Investigative Dermatology* (2021), doi: https://doi.org/10.1016/j.jid.2021.03.015.

This is a PDF file of an article that has undergone enhancements after acceptance, such as the addition of a cover page and metadata, and formatting for readability, but it is not yet the definitive version of record. This version will undergo additional copyediting, typesetting and review before it is published in its final form, but we are providing this version to give early visibility of the article. Please note that, during the production process, errors may be discovered which could affect the content, and all legal disclaimers that apply to the journal pertain.

© 2021 The Authors. Published by Elsevier, Inc. on behalf of the Society for Investigative Dermatology.

Journal Pre-proof

TITLE PAGE

Mechanisms of broad-band ultraviolet B irradiation-induced itch in mice

Liang Cao[1,*], Xueping Yue[1,*], Yonghui Zhao[1,*], Lixia Du[1], Zili Xie[1], Yi Yuan[1], Sha Zhang[2], Feng Li[2], Jing Feng[1,#], Hongzhen Hu[1]

1 Department of Anesthesiology, The Center for the Study of Itch & Sensory Disorders, Washington University School of Medicine, St. Louis, MO, USA

2 Department of Basic Medicine, Shaanxi University of Chinese Medicine, XianYang, Shaanxi, China

The work was performed at Washington University School of Medicine, Department of Anesthesiology, The Center for the Study of Itch & Sensory Disorders, St. Louis, MO, USA.

* These authors contributed equally to this work.

Corresponding to: Jing Feng, jingfeng@wustl.edu, Department of Anesthesiology, The Center for the Study of Itch & Sensory Disorders, Washington University School of Medicine, St. Louis, MO, USA.

Short title: TRPV1 mediates BB-UVB-induced itch

Abbreviations:

BB-UVB: Broad-band UVB

DRG: Dorsal root ganglion

NB-UVB: Narrow-band UVB

NSAID: Nonsteroidal anti-inflammatory drug

PBS: Phosphate-buffered saline

RTX: Resiniferotoxin

SNI: Spared nerve injury

TRPA1: Transient receptor potential cation channel subfamily A member 1

TRPV1: Transient receptor potential cation channel subfamily V member 1

UV: Ultraviolet

wt: Wild-type

Journal Pre-proof

Mechanisms of broad-band ultraviolet B irradiation-induced itch in mice

Abstract

Although sunburn can produce severe uncontrollable itching, the underlying mechanisms of ultraviolet (UV) irradiation-induced itch are poorly understood because of a lack of experimental animal models of sunburn itch. Here we established a sunburn-related mouse model and found that Broad-band UVB (BB-UVB) irradiation elicited scratching but not wiping behavior in mice. By using a combination of live-cell Ca^{2+} imaging and quantitative RT-PCR on dorsal root ganglion (DRG) neurons, hematoxylin and eosin staining, immunofluorescence staining of skin preparations, behavioral testing, in combination with genetic and pharmacological approaches, we showed that TRPV1-positive DRG neurons but not mast cells are involved in BB-UVB irradiation-induced itch. Moreover, both genetic and pharmacological inhibition of TRPV1 function significantly alleviated BB-UVB irradiation-induced itch response. Collectively, our results suggest that BB-UVB irradiation evokes itch sensation in mice through promoting TRPV1 channel function in DRG neurons and provide potential therapeutic targets for sunburn-related itch.

Keywords: Sunburn-related itch; BB-UVB; TRPV1; Itch model

Journal Pre-proof

Journal Pre-proof

Introduction

Sunburn or ultraviolet (UV) dermatitis, often occurring in vacationers and farmers, is a skin phototoxic reaction to UV radiation, which is generally associated with erythema, pustules, heat sensitization, followed by tanning and epidermal thickening (Han and Maibach, 2004). Besides skin inflammation, sunburn-related itch, also known as the hell's itch (Wilder-Smith, 2019; Berry, 2018), is a debilitating condition which can severely impair quality of life. Due to a lack of experimental animal models, the molecular and cellular mechanisms of sunburn-related itch remain largely unknown.

The most common form of UV radiation is sunlight, which produces three types of UV rays: UVA, UVB and UVC (Supplementary Figure S1) (Gupta et al., 2013). Because UVC is absorbed by ozone, ambient sunlight is predominantly long-wavelength UVA (320-400 nm) (90%–95%) and short-wavelength UVB (290-320 nm) (5%–10%) (Tuchinda et al., 2007). It has been shown that UVA could penetrate deeply into the dermis, promoting the production of early melanin synthesis through activation of the cation channel transient receptor potential ankyrin 1 (TRPA1) (Bellono et al., 2013). On the other hand, UVB is primarily absorbed by the epidermis. Although narrow-band UVB (NB-UVB, ~311 nm) was reported to cause sunburn-induced pain sensation by activating keratinocyte-expressed TRPV4 channel (Moore et al., 2013), NB-UVB phototherapy is widely used for the treatment of psoriasis, atopic dermatitis, and

vitiligo. However, the role of broad-band UVB (BB-UVB, 290-320 nm) in the setting of sunburn-related skin damage remains unclear.

In the present study, we first established a mouse model of sunburn-related itch. We found that BB-UVB irradiation selectively promoted the function of TRPV1 expressed by primary sensory neurons to induce an itch-associated scratching behavior in mice. These findings identify TRPV1 as a potential drug target for the treatment of UVB irradiation-induced itch.

Results

BB-UVB irradiation evokes an itch-associated behavior in mice

To investigate whether BB-UVB exposure promotes pathological skin conditions, we irradiated wild-type (wt) C57BL/6J mice on day 0 with different doses of BB-UVB (Figure 1a). Surprisingly, compared with white-light irradiated group, a single exposure to BB-UVB irradiation with power ≥ 400 mJ/cm^2 on the nape of the neck area was able to elicit a robust scratching behavior in mice, reaching a plateau

After confirming that BB-UVB elicited a robust scratching behavior in mice, we next determined whether this behavior resulted from pain or itch by using the well-established cheek model (Spradley et al., 2012). Surprisingly, when exposed to mouse cheek, BB-UVB irradiation (800 mJ/cm^2) selectively produced a robust itch-associated scratching by a hind paw but not pain-associated wiping by a forelimb towards the site of irradiation (Figure 2a-c). In agreement with this finding, the BB-UVB irradiation-induced scratching behavior was selectively suppressed by an anti-pruritic μ-opioid receptor antagonist, naltrexone (Figure 2d), but not ibuprofen, a pain-inhibiting nonsteroidal anti-inflammatory drug (NSAID) (Figure 2e). In marked contrast, exposure of the NB-UVB irradiation (800 mJ/cm^2)

Journal Pre-proof

immune cells mediates acute/chronic itch in multiple mouse models of itch (Luo et al., 2018; Chen et al., 2016). To determine whether these TRP channels are also involved in BB-UVB-induced itch, we tested BB-UVB irradiation on mice deficient in Trpa1, Trpv1 or Trpv4. Interestingly, genetic ablation of Trpv1 function readily abolished BB-UVB-induced itch, whereas a deficiency in Trpa1 or Trpv4 had negligible effect on BB-UVB-induced scratching behavior (Figure 3a). In agreement with this observation, subcutaneous injection of resiniferotoxin (RTX), a super potent TRPV1 activator that ablates TRPV1-expressing ($TRPV1^+$) primary sensory afferents (Riol-Blanco et al., 2014), markedly reduced BB-UVB-induced scratching when compared with vehicle-treated mice (Figure 3b and). Furthermore, both preventative and acute pharmacological inhibition of TRPV1 function by AMG9810, a specific TRPV1 antagonist, effectively suppressed BB-UVB-induced itch in both initiation and plateau phases (Figure 3c and d). These findings strongly suggest that TRPV1 channel function is required for BB-UVB-induced itch sensation and inhibition of TRPV1 function might be a promising strategy for the treatment of sunburn-related itch.

TRPV1 is dispensable in BB-UVB-induced inflammation

Bi-directional interactions between cutaneous immune cells and sensory nerve endings are a unique paradigm contributing to both skin inflammation and chronic itch (Oetjen et al., 2017; Feng et al., 2017). Interestingly, UV stimulation of dermal

mast cells was shown to be a key event leading to UV-induced inflammation (Sarchio et al., 2012). To determine whether this bidirectional positive feedback loop is also involved in BB-UVB-induced itch, we tested BB-UVB-induced scratching behavior in mast cell-deficient $Kit^{W\text{-}sh}$ "sash" mice. Surprisingly, no significant difference was found in the BB-UVB-induced scratching responses between the "sash" mice and the wt mice (Figure 4a). Moreover, although the skin thickness was significantly increased in both Trpv1-deficient mice and wt mice treated with BB-UVB irradiation when comparing with the sham group, no significant difference in skin histology or skin lesion scores was found between these two groups (Figure 4b-d). Together, these results suggest that TRPV1 function is not involved in BB-UVB-induced skin inflammation and the neural-mast cell interaction is dispensable for BB-UVB-induced persistent itch in mice.

BB-UVB sensitizes $TRPV1^{+}$ DRG neurons

Having provided convincing data showing that BB-UVB irradiation-induced itch was TRPV1-dependent, we next investigated the potential mechanism underlying TRPV1 activation after BB-UVB irradiation. To test the possibility that TRPV1 may be directly activated by BB-UVB irradiation, we performed whole-cell patch-clamp recording on HEK293 cells transiently transfected with mouse TRPV1 plasmid. Surprisingly, BB-UVB irradiation did not activate detectable current while capsaicin induced a TRPV1-dependent current (Supplementary Figure S4). Furthermore, TRPV1 activation was not a consequence of BB-UVB

irradiation-induced temperature increase in the skin as we showed that the skin temperature was not significantly changed in the absence and in the presence of BB-UVB irradiation (**Supplementary Figure S5**).

Alternatively, up-regulation of neuronal TRPV1 expression and function might contribute to BB-UVB-induced itch. To test this hypothesis, we freshly isolated and cultured DRG neurons innervating the irradiated skin area 3 days after BB-UVB irradiation and measured the expression of itch-related TRP channel genes using real-time PCR. BB-UVB irradiation led to a dramatic increase in the expressions of Trpv1 and Trpa1 while the expressions of Trpv3, Trpv4, Trpc4 and Trpm8 were comparable between the BB-UVB irradiation group and the sham control group (Fig**ure 5a**). This finding prompted us to investigate if BB-UVB irradiation promotes TRPV1 function in DRG neurons using live-cell Ca^{2+} imaging since we have shown that TRPV1 but not TRPA1 is essential to BB-UVB-induced itch. Indeed, the proportion of DRG neurons responded to a low concentration (10 nM) of TRPV1 agonist capsaicin was significantly larger in the BB-UVB-irradiated mice when compared with sham control mice, although higher concentrations of capsaicin (100 and 300 nM) evoked Ca^{2+} responses in comparable numbers of DRG neurons in both groups (Fig**ure 5b and Supplementary Figure S6**). Taken together, these data suggested that up-regulation of the expression and function of TRPV1 is critically involved in BB-UVB irradiation-induced sensitization of pruriceptors, leading to itch-associated scratching.

It should be noted that TRPV1 expression was not affected until day 3 (**Supplementary Figure S7**). On the other hand, we did observe an increased proliferation of keratinocytes and infiltration of macrophages starting from day 0 (**Supplementary Figure S8**), suggesting a potential epidermal factor/immune cell-mediated sensitization of TRPV1 function in the early stage and upregulation of TRPV1 expression in the late stage in BB-UVB-induced itch signaling.

Discussion

In the present study, we established a mouse model of UV irradiation-induced itch and demonstrated that acute exposure to BB-UVB promotes TRPV1 expression and function, leading to itch-associated scratching behavior in mice. The inhibition of TRPV1 function by either pharmacological or genetic approach is sufficient to alleviate BB-UVB-induced itch. Collectively, these findings provide a unique mouse model for the study of BB-UVB irradiation-related itch and identify a cellular mechanism of UV irradiation-induced itch in the periphery.

Although pathological skin conditions caused by excessive UV exposure have been described at length, most of the studies focused on the effects of UV irradiation on epidermal keratinocytes and immune cells. For instance, UV irradiation caused DNA damage in keratinocytes (de Pedro et al., 2018) and suppressed cell-mediated immune function, resulting in the development of skin cancer and susceptibility to infectious diseases (Kelly et al., 2000). Interestingly, we found that RTX-treated

mice showed fewer scratching bouts when compared with the vehicle-treated mice after BB-UVB irradiation, suggesting that BB-UVB irradiation may also affect primary sensory nerves that are critical to the initiation of both pain and itch.

Recent exciting studies have significantly advanced our knowledge about the important roles of TRP channels in the development of UV irradiation-related skin diseases. For instance, epidermal-expressing TRPV4 channel was reported to mediate the NB-UVB-induced pain behavior in mice (Moore et al., 2013). TRPC7 channels mediate UVB-induced Ca^{2+} influx which is important to skin aging and tumor development (Hsu et al., 2020). Moreover, Lee et al showed that $TRPV1^{+}$ nerve is significantly increased in aged and photoaged human skin (Lee et al., 2009). Consistent with these studies, we also found that the expression level of TRPV1 but not TRPV3, TRPV4, TRPC4 and TRPM8 channels was upregulated in individual DRG neurons, leading to a much higher percentage of DRG neurons from BB-UVB-irradiated mice responsive to a low concentration of capsaicin when compared with the sham group. Interestingly, the percentage of TRPV1-responsive neurons to 300 nM capsaicin were comparable between naive, sham group and BB-UVB-irradiated group at day 3, suggesting an up-regulation in TRPV1 expression rather than an expansion $TRPV1^{+}$ neurons upon BB-UVB irradiation. Although TRPA1 expression was also increased in the DRG neurons by BB-UVB-irradiation, TRPA1 knockout mice didn't show any reduction in itch behavior after BB-UVB-irradiation. Interestingly, Bellono et al showed that TRPA1

is expressed by human melanocytes and can be directly activated by UVA, contributing to enhanced pigmentation through upregulation of melanin synthesis (Bellono et al., 2013). It will be interesting to investigate whether BB-UVB-induced activation of neuronal TRPA1 is involved in skin pigmentation through neuron-melanocyte interaction in mice in future studies.

It is well-established that neural-immune interaction has been involved in the development of itch sensation (Wang et al., 2020). For example, activation of $TRPV1^{+}$ nociceptors by house dust mites promotes mast cell degranulation that drives allergic itchy skin diseases (Serhan et al., 2019). However, we observed no reduction in BB-UVB-induced scratching behavior in mast cell-deficient mice, suggesting that mast cells are unlikely involved in the development of BB-UVB-induced itch. Moreover, although TRPV1 is indispensable for BB-UVB-induced itch, it is not required for BB-UVB-induced inflammation, further suggesting that distinct molecular and cellular mechanisms might be involved in itch and skin inflammation produced by BB-UVB irradiation.

Although we showed that TRPV1 is involved in BB-UVB irradiation-induced itch in mice, the mechanisms underlying TRPV1 activation by BB-UVB irradiation remain unclear. There are at least two possibilities: Firstly, TRPV1 channel may be directly activated by BB-UVB irradiation. However, BB-UVB irradiation could not evoke TRPV1-mediated current. Moreover, the skin temperature was not significantly affected by BB-UVB irradiation . Indeed, Baumbauer et al showed

that optogenetic activation of keratinocytes evoked action potential firing in various types of skin sensory fibers (Baumbauer *et al*., 2015); Oetjen et al also showed that type 2 cytokines released from immune cells could activate sensory neurons in both mice and humans (Oetjen *et al*., 2017), indicating the possibility that TRPV1-expressing fibers may be activated by the neurotrophins/cytokines released from keratinocytes/immune cells upon BB-UVB irradiation. Consistent with this hypothesis, we found accumulation of macrophages and increased proliferation of keratinocytes starting from day 0 to day 3, which was correlated with the scratching behavior in the BB-UVB-irradiated mice. Taken all these data together, we speculated that TRPV1 may function as the downstream target of keratinocytes/immune cells and mediate BB-UVB-induced itch sensation rather than a direct activation by BB-UVB irradiation. More studies with pharmacological/genetic approaches are required to clarify the epithelia-neuronal and/or immune-neuronal crosstalk underlying BB-UVB-induced activation of TRPV1 in the future.

In summary, we showed that BB-UVB-irradiation induces itch sensation in mice through promoting the expression and function of the sensory neuron-expressed TRPV1 channel. Identification of TRPV1 as the itch mediator in BB-UVB-induced itch will not only advance our understanding of the cellular and molecular basis of sunlight-induced itch sensation but also should facilitate the development of TRPV1-based therapeutics for UV-irradiation-related itch management.

Materials & Methods

Animals

Adult C57BL/6J (Jackson Laboratories), Trpv1$^{-/-}$ (Jackson Laboratories), Trpa1$^{-/-}$ (Jackson Laboratories), Trpv4$^{-/-}$ (Suzuki et al., 2003) and mast cell deficient Kit^{Wsh} "sash" mice (Jackson Laboratories) were used in this study. All the transgenic mice were backcrossed with C57BL/6J mice for more than ten generations. Both male and female mice were used in the study as no sex difference was observed. All mice were housed under a 12-hour light/dark cycle with free access to food and water. All experiments were approved by the Animal Studies Committee at Washington University School of Medicine and were performed in accordance with the guidelines of the National Institutes of Health and the International Association for the Study of Pain.

Mouse model of UV irradiation

The side area designated for UV stimulation was shaved from the nape of the neck to the lateral abdomen. Mice were acclimated for one hour in 2 consecutive days by placing them individually in a recording chamber. On the third day, mice were videotaped and hindpaw scratching bouts were counted as baseline (Figure 1a lower panel). On the day of experiment (marked as day 0), mice were anaesthetized by 2% isoflurane inhalation. The UV photo-therapy device (SolRx 100-Series, Solarc Systems, Ontario, CAN) was placed on the top of the round gasket, allowing

circular light stimulation only to the shaved skin area (Figure 1a upper panel). After a specific dose of UV irradiation, mice were immediately videotaped, and the number of scratching/wiping bouts was counted. The skin surface temperature was tested with a digital thermal meter and no significant temperature changes were detected during the irradiation process (Supplementary Figure S5), excluding the possibility of thermal activation of TRPV1 by UV irradiation. A digital UV meter (Solarmeter, Queensland, AUS) was used to measure the UV power density. The irradiation dose (mJ) was determined by the following formula: UV intensity (5 mw/cm^2) × exposure time × exposure area (1 cm^2 for each mouse). In our study, the UVB intensity, which was measured by UV meter, is 5mW/cm^2. The times required to reach the dose of 200 mJ, 400 mJ, 800 mJ and 1600 mJ were 40 s, 80 s, 160 s, 320 s, respectively. The power density of the UVA is 3 mw/cm^2, the times required to reach the dose of 200 mJ, 1000 mJ, 2000 mJ, 6000 mJ were 67 s, 333 s, 667 s and 2000 s, respectively.

Three types of UV short compact fluorescent lamps were used in this study. BB-UVB lamp (a two pin 9-watt type (PHILIPS pl-s9w/12/2p)) emits light in a broad range over the UVB spectrum, including the shorter wavelengths responsible for sunburn. Narrow band (NB)-UVB tube (PHILIPS pl-s9w/01/2p) only generates UVB-narrowband at 311 nm and has fewer clinically burning incidents than BB-UVB. According to manufacturer's introduction, BB-UVB is considered a more aggressive UV-light therapy than NB-UVB and has a much greater skin-burning

potential. A two pin 9-watt bulb (PHILIPS pl-s9w/10/2p) was used to deliver harmful UVA radiation (320 to 400 nm).

Mouse cheek model

The right cheek of mice was shaved and acclimated for at least two days before irradiation. At day 0, a dose of 800 mJ UVB shines on the cheek through a smaller circular hole of the gasket. All mice were videotaped for one hour and the scratching/wiping bouts were counted. The discrimination of wiping, scratching and grooming behavior refers to previous authoritative study (Akiyama et al., 2010).

Drug administration

The analgesic drug ibuprofen (Sigma-Aldrich, St. Louis, MO) and antipruritic drug naltrexone (Sigma-Aldrich) were administrated through i.p. injection into the mice on day 0. Forty minutes later, the mice were exposed to UVB stimulation. From day 1 to day 7, these drugs were repeatedly given. All mice were videotaped for one hour and the corresponding scratching bouts were counted. AMG9810 (Tocris Bioscience, Bristol, UK) was dissolved in DMSO and diluted with 0.9% saline before use. Preventative and therapeutic application of 0.003 mg/kg AMG9810 was started from day 0 and 3, respectively.

Quantitative RT-PCR

Total RNA was extracted from freshly isolated mouse DRG neurons by RNeasy kit (Qiagen, Germantown, MD) according to the instructions. RNA was treated with

DNase I (Invitrogen, Carlsbad, California) and the cDNA was synthesized in vitro using ThermoScript RT–PCR System kit (Invitrogen). Reactions were carried out in a volume of 20 μl per reaction containing 10 μl Fast SYBR™ Green Master Mix (Applied Biosystems, Foster City, CA), 0.5 μl cDNA, 1.2 μl 5 μM primer mix, and 8.3 μl ddH_2O using StepOnePlus real-time PCR system (Applied Biosystems, Foster City, CA). Relative mRNA levels of different target genes referenced to GAPDH were calculated using $2^{-\Delta\Delta Ct}$ methods. Primer sequences used for each gene were selected from pre-validated PrimeTime qPCR assays (Integrated DNA Technologies, Coralville, Iowa). Primer sequences (5' to 3') of each gene were listed as following:

mTRPV1 F: ACCACGGCTGCTTACTATCG

R: TCCCCAACGGTGTTATTCAG

mTRPV4 F: CCTGCTGGTCACCTACATCA

R: CTCAGGAACACAGGGAAGGA

mTRPA1 F: CCATGACCTGGCAGAATACC

R: TGGAGAGCGTCCTTCAGAAT

mTRPM8 F: GCTGCCTGAAGAGGAAATTG

R: GCCCAGATGAAGAGAGCTTG

mTRPV3 F: TGACATGATCCTGCTGAGGAGTG

R: ACGAGGCAGGCGAGGTATTCTT

mTRPC4 F: CGACCATGCAGATATAGAATGGAA

R: TGGTATTGGTGATGTCTTCTCAAG

GAPDH F: GCACAGTCAAGGCCGAGAAT

R: GCCTTCTCCATGGTGGTGAA

Chemical ablation of TRPV1$^+$ sensory nerves

Resiniferatoxin (RTX) (Sigma-Aldrich), a capsaicin analog, was injected subcutaneously into 4-week-old mice at three increasing doses (30, 70, and 100 μg/kg) for 3 consecutive days as we have described (Feng *et al*., 2017). Vehicle group was treated with vehicle solution (DMSO in PBS). Mice were allowed to rest for 6 weeks before behavioral test. The effectiveness of RTX ablation of TRPV1+ primary afferents was validated by the tail flick assay (Supplementary **Figure S3**).

Isolation and short-term culture of mouse DRG neurons

Mice were sacrificed three days after BB-UVB irradiation. The vertebral column corresponding to the stimulated skin area was removed and placed in ice-cold HBSS. DRG neurons were then acutely dissociated and transferred to 1 ml dispase/collagenase Type I mixture containing 4 U/ml dispase, 342 U/ml collagenase I in pre-warmed 1 x HBSS without phenol red, and incubated at 37°C for 30 min. After incubation, the solution was centrifuged, and the liquid

supernatant was discarded. The DRG neurons were re-suspended in neural culture medium containing 2% B-27 supplement, 1% L-glutamine, 100 U/mL penicillin, 100 ug/mL streptomycin, and 50 ng/mL nerve growth factor. Then, the neurons were placed on a 5-mm coverslip coated with poly-L-lysine (10 μg/mL) and cultured under a humidified atmosphere of 5% CO_2 /95% air at 37°C for 18 to 24 h before further experiment.

Live-cell Ca^{2+} imaging

Fura-2-based ratiometric measurement of $[Ca^{2+}]i$ was performed as we have previously described (Feng et al., 2017). DRG neurons were loaded with 4 μM Fura-2 AM (Life Technologies, Grand Island, NY) in culture medium at 37°C for 60 min. Cells were then washed 3 times in wash buffer (1 L wash buffer containing: HBSS 20 x 50 ml, $CaCl_2$ 2M x 1 ml, HEPES 2.38 g, and glucose 1.8 g, sucrose 10.26 g, pH 7.40) and incubated in HBSS at room temperature for 30 min before use. Fluorescence at 340 and 380 nm excitation wavelengths was recorded on an inverted Nikon Ti-E microscope and NIS-Elements imaging software (Nikon Instruments Inc, Melville, NY). Fura-2 ratios (F340/F380) reflecting the change in intracellular Ca^{2+} upon stimulation were recorded. Values were obtained from 100 to 250 cells in time-lapse images from each coverslip. The threshold of cellular activation was defined as 20% above the baseline.

HEK293 cell culture and transfection

HEK 293 cells were grown as a monolayer using passage numbers less than 30 and maintained in DMEM (Life Technologies, Carlsbad, CA, USA), supplemented with 10% FBS (Life Technologies), 100 U mL^{-1} penicillin, and 100 µg mL^{-1} streptomycin in a humidified incubator at 37°C with 5% CO_2. The cells were transiently transfected with a cDNA for mouse TRPV1 (mTRPV1) using Lipofectamine 2000 (Invitrogen, Carlsbad, CA, USA) with a ratio of 0.8:2. Following transfection, the cells were maintained in DMEM at 37°C for 24 h before use.

Patch-clamp recordings

Whole-cell patch-clamp recordings were performed using an Axon 700B amplifier (Molecular Devices, Sunnyvale, CA, USA) at room temperature (22–24°C) on the stage of an inverted phase-contrast microscope equipped with a filter set for GFP visualization. Pipettes pulled from borosilicate glass (BF 150-86-10; Sutter Instrument, Novato, CA, USA) with a Sutter P-1000 pipette puller had resistances of 2-4 MΩ, when filled with pipette solution containing 140 mM CsCl, 2 mM EGTA and 10 mM HEPES with pH 7.3 and 315 mOsm L^{-1} osmolarity. The whole-cell membrane currents were recorded using voltage ramps from −100 to +100 mV for 500 ms at a holding potential of 0 mV. Data were acquired using Clampex 10.4 software (Molecular Devices). Currents were filtered at 2 kHz and digitized at 10 kHz. Data were analyzed and plotted with Clampfit 10 (Molecular Devices).

Skin lesion score

The severity of BB-UVB induced mouse skin lesion was assessed using the standard scores of Leung (Leung, 1997). In brief, symptoms of itch (erythema, edema, scarring, and decrustation) were evaluated. Each sign was graded from 0 to 3 (none, 0; mild, 1; moderate, 2; severe, 3). The total score is defined as the sum of the individual scores, which ranges from 0 to 12.

Histological evaluation of skin lesion

Mouse skin was harvested and then fixed in 4% paraformaldehyde in phosphate-buffered saline (PBS), dehydrated in 30% sucrose, and embedded in OCT. The tissue was cut into twelve-micron sections in a Leica CM1950 cryostat (Leica Biosystems, Buffalo Grove, IL). Hematoxylin and Eosin staining was performed according to standard protocols. After the imaging is completed, the Image-Pro Plus 6.0 analysis software is used. The pixel was uniformly used as the standard unit to measure the thickness of the 5 epidermis randomly selected in each slice. Each group contains 3 HE slices from 3 mice.

Spared Nerve Injury (SNI) model

C57BL/6J mice were subjected to peripheral neuropathy induced by SNI operation (Liu et al., 2015). In brief, the mice were anesthetized and the biceps femoris muscle was exposed. A section was made through the biceps femoris to further expose the sciatic nerve and its three terminal branches: the sural, common peroneal, and tibial

nerves. The common peroneal and tibial nerves were tightly ligated with 6.0 silk suture. The nerve stump distal to the ligation was removed (2 to 4 mm). The muscle and skin were then separately closed. For sham surgery, the sciatic nerve was exposed as described above, with no operations on the nerve. And the measurement of mechanical pain threshold was tested via *Von* Frey test.

Data Availability Statement

Datasets related to this article can be found at http://dx.doi.org/10.17632/zjhv332x 2.1, hosted at Mendeley Data.

ORCiDs

Liang Cao: https://orcid.org/0000-0002-4739-4145

Xueping Yue: https://orcid.org/0000-0003-1222-2535

Yonghui Zhao: https://orcid.org/0000-0002-6192-4130

Lixia Du: https://orcid.org/0000-0002-8578-8268

Zili Xie: https://orcid.org/0000-0002-9060-6780

Yi Yuan: https://orcid.org/0000-0001-8828-990X

Sha Zhang: https://orcid.org/0000-0003-1175-6770

Feng Li: https://orcid.org/0000-0003-2385-3746

Jing Feng: https://orcid.org/0000-0001-6726-7912

Journal Pre-proof

Hongzhen Hu: https://orcid.org/0000-0002-8967-7522

Conflict of Interest Statement

Authors have no potential conflict of interest to disclose.

Acknowledgments

This work was supported partly by grants from the National Institutes of Health, R01AA027065, R01AR077183, and R01DK103901 (to H. H.), The Center for the Study of Itch & Sensory Disorders and the Department of Anesthesiology at Washington University School of Medicine to H. H.

Author Contributions Statement

Conceptualization: HZH and JF; Data curation: LC, XPY, YHZ, LXD; Formal Analysis: LC, XPY, YHZ, LXD, YY, SZ, FL; Funding Acquisition: HZH; Investigation: LC, XPY, YHZ, LXD, SZ; Methodology: LC, XPY, YHZ, LXD; Project Administration: HZH and JF; Resources: HZH; Supervision: HZH and JF; Writing-Original Draft Preparation: JF, LC and HZH; Writing-Review and Editing: JF, LC and HZH.

Journal Pre-proof

References:

Akiyama T, Carstens MI, Carstens E (2010) Differential itch- and pain-related behavioral responses and micro-opoid modulation in mice. Acta Derm Venereol 90 :575-581.

Baumbauer KM, DeBerry JJ, Adelman PC, Miller RH, Hachisuka J, Lee KH, et al. (2015) Keratinocytes can modulate and directly initiate nociceptive responses. ELIFE 4.

Bellono NW, Kammel LG, Zimmerman AL, Oancea E (2013) UV light phototransduction activates transient receptor potential A1 ion channels in human melanocytes. Proc Natl Acad Sci U S A 110 :2383-2388.

Berry J (2018) Sunburn and hell's itch: How to get relief. MEDICAL NEWS TODAY 3 :19.

Chen Y, Fang Q, Wang Z, Zhang JY, MacLeod AS, Hall RP, et al. (2016) Transient Receptor Potential Vanilloid 4 Ion Channel Functions as a Pruriceptor in Epidermal Keratinocytes to Evoke Histaminergic Itch. J BIOL CHEM 291 :10252-10262.

de Pedro I, Alonso-Lecue P, Sanz-Gomez N, Freije A, Gandarillas A (2018) Sublethal UV irradiation induces squamous differentiation via a p53-independent, DNA damage-mitosis checkpoint. CELL DEATH DIS 9 :1094.

Feng J, Luo J, Mack MR, Yang P, Zhang F, Wang G, et al. (2017) The antimicrobial peptide human beta-defensin 2 promotes itch through Toll-like receptor 4 signaling in mice. J Allergy Clin Immunol 140 :885-888.

Feng J, Yang P, Mack MR, Dryn D, Luo J, Gong X, et al. (2017) Sensory TRP channels contribute differentially to skin inflammation and persistent itch. NAT COMMUN 8 :980.

Gupta A, Avci P, Dai T, Huang YY, Hamblin MR (2013) Ultraviolet Radiation in Wound Care: Sterilization and Stimulation. Adv Wound Care (New Rochelle) 2 :422-437.

Han A, Maibach HI (2004) Management of acute sunburn. AM J CLIN DERMATOL 5 :39-47.

Hsu WL, Tsai MH, Wu CY, Liang JL, Lu JH, Kahle JS, et al. (2020) Nociceptive transient receptor potential canonical 7 (TRPC7) mediates aging-associated tumorigenesis induced by ultraviolet B. AGING CELL 19:e13075.

Kelly DA, Young AR, McGregor JM, Seed PT, Potten CS, Walker SL (2000) Sensitivity to sunburn is associated with susceptibility to ultraviolet radiation-induced suppression of cutaneous cell-mediated immunity. J EXP MED 191 :561-566.

Lee YM, Kim YK, Chung JH (2009) Increased expression of TRPV1 channel in intrinsically aged and photoaged human skin in vivo. EXP DERMATOL 18 :431-436.

Leung DY (1997) Atopic dermatitis: immunobiology and treatment with immune modulators. CLIN EXP IMMUNOL 107 Suppl 1 :25-30.

Liu S, Mi WL, Li Q, Zhang MT, Han P, Hu S, et al. (2015) Spinal IL-33/ST2 Signaling Contributes to Neuropathic Pain via Neuronal CaMKII-CREB and Astroglial JAK2-STAT3 Cascades in Mice. ANESTHESIOLOGY 123 :1154-1169.

Luo J, Feng J, Yu G, Yang P, Mack MR, Du J, et al. (2018) Transient receptor potential vanilloid 4-expressing macrophages and keratinocytes contribute differentially to allergic and nonallergic chronic itch. J Allergy Clin Immunol 141 :608-619.

Moore C, Cevikbas F, Pasolli HA, Chen Y, Kong W, Kempkes C, et al. (2013) UVB radiation generates sunburn pain and affects skin by activating epidermal TRPV4 ion channels and triggering endothelin-1 signaling. Proc Natl Acad Sci U S A 110:E3225-E3234.

Oetjen LK, Mack MR, Feng J, Whelan TM, Niu H, Guo CJ, et al. (2017) Sensory Neurons Co-opt Classical Immune Signaling Pathways to Mediate Chronic Itch. CELL 171 :217-228.

Riol-Blanco L, Ordovas-Montanes J, Perro M, Naval E, Thiriot A, Alvarez D, et al. (2014) Nociceptive sensory neurons drive interleukin-23-mediated psoriasiform skin inflammation. NATURE 510 :157-161.

Sarchio SN, Kok LF, O'Sullivan C, Halliday GM, Byrne SN (2012) Dermal mast cells affect the development of sunlight-induced skin tumours. EXP DERMATOL 21 :241-248.

Serhan N, Basso L, Sibilano R, Petitfils C, Meixiong J, Bonnart C, et al. (2019) House dust mites activate nociceptor-mast cell clusters to drive type 2 skin inflammation. NAT IMMUNOL 20 :1435-1443.

Spradley JM, Davoodi A, Carstens MI, Carstens E (2012) Opioid modulation of facial itch- and pain-related responses and grooming behavior in rats. Acta Derm Venereol 92 :515-520.

Suzuki M, Mizuno A, Kodaira K, Imai M (2003) Impaired pressure sensation in mice lacking TRPV4. J BIOL CHEM 278 :22664-22668.

Tuchinda C, Lim HW, Strickland FM, Guzman EA, Wong HK (2007) Comparison of broadband UVB, narrowband UVB, broadband UVA and UVA1 on activation of apoptotic pathways in human peripheral blood mononuclear cells. Photodermatol Photoimmunol Photomed 23 :2-9.

Wang F, Yang TB, Kim BS (2020) The Return of the Mast Cell: New Roles in Neuroimmune Itch Biology. J INVEST DERMATOL 140 :945-951.

Wilder-Smith AJ (2019) Hell's itch due to sunburn. J TRAVEL MED 26.

Xie Z, Hu H (2018) TRP Channels as Drug Targets to Relieve Itch. Pharmaceuticals (Basel) 11:100.

Figure Legends

Figure 1. BB-UVB irradiation evokes scratching behavior in mice. (a) Diagram illustrating the device and experimental protocol used for the generation of a mouse model of UV irradiation-induced itch. Upper panel: The UV-emitting device (1) targeting a small skin area is placed on the metal shelf (2) and parallel to the shading gasket (3), which ensures that the UV light source can only pass through the circular hole on the gasket with an area of 1 cm^2. This design enables the circular frame aligned with the circular hole on top of the mouse back skin. Lower panel: The time course used to generate the mouse model of UV irradiation-induced itch. (b) Dose and time-dependent scratching responses in mice irradiated by BB-UVB irradiation. n = 5 for 1600 mJ/cm^2, 800 mJ/cm^2 and 400 mJ/cm^2 group, n = 6 for 200 mJ/cm^2 and sham group. (c) UVA irradiation did not induce scratching in mice. n = 5 for each group. (d) NB-UVB (800 mJ/cm^2) induced a short-lived scratching response in mice. n = 5 for each group. All data were expressed as mean ± SEM. *p < 0.05, **p < 0.01, ***p < 0.001, two-way ANOVA with post hoc Bonferroni test.

Figure 2. BB-UVB irradiation evokes itch but not pain sensation. (a-b) Hindpaw scratching (a) and forepaw wiping (b) behaviors induced by BB-UVB irradiation on the cheek of mice. n = 6 for BB-UVB group, n= 5 for sham group. (c) Representative image showing a typical hindpaw scratching behavior in a mouse after BB-UVB irradiation on the cheek. (d-e) BB-UVB-evoked scratching in mice treated with naltrexone (10 mg/kg) (d), n = 11 for each group or ibuprofen (150 mg/kg) (e), n = 12 for each group. (f-g) Scratching (f) and wiping (g) behaviors evoked by NB-UVB irradiation on the cheek of mice. n = 5 for each group. (h) NB-UVB-induced wiping behavior in mice treated with vehicle or ibuprofen (150 mg/kg). n = 5 for each group. (i) SNI-induced neuropathic pain behavior in mice treated with ibuprofen (150 mg/kg) or vehicle. n = 5 for each group. All data were presented as mean ± SEM and analyzed with two-way ANOVA with post hoc Bonferroni test. *p < 0.05, **p < 0.01, ***p < 0.001, ns, not significant.

Figure 3. TRPV1 mediates BB-UVB-induced itch. (a) BB-UVB-induced scratching behavior in wt, Trpv1$^{-/-}$, Trpa1$^{-/-}$ and Trpv4$^{-/-}$ mice. n = 12 for wt (C57BL/6J), n = 11 for Trpv1$^{-/-}$, n = 14 for Trpa1$^{-/-}$, n = 14 for Trpv4$^{-/-}$. All mice were backcrossed to the C57BL/6J background for more than 10 generations. (b) BB-UVB-induced scratching in mice treated with vehicle or RTX. n = 10 for vehicle group, n = 12 for RTX group. (c-d) BB-UVB-induced scratching in mice treated with AMG9810 (0.003 mg/kg) or vehicle starting from Day 0 (c, n = 7 for AMG9810 group, n = 9 for vehicle group) (preventative) or Day 3 (d, n = 6 for AMG9810 group, n = 10 for vehicle group) (acute inhibition). All data were presented as mean ± SEM and analyzed with two-way ANOVA with post hoc Bonferroni test. *p < 0.05, **p < 0.01, ***p < 0.001.

Figure 4. TRPV1 is not involved in BB-UVB-induced skin inflammation and mast cell-deficiency does not affect BB-UVB-induced persistent itch. (a) BB-UVB-induced scratching in wt littermate control and mast cell-deficient sash mice. n = 7 for each group. ns, not significant, two-way ANOVA with post hoc Bonferroni test. (b) BB-UVB-induced skin lesion score between wt and Trpv1$^{-/-}$ mice. n = 6 for wt group, n = 6 for Trpv1$^{-/-}$ group. ns, not significant (c) Statistical analysis of the relative epidermal thickness in wt, Trpv1$^{-/-}$, and sham groups. All data were presented as mean ± SEM and analyzed with Student t test. ***p < 0.001, ns, not significant. (d) Representative histological images from wt, Trpv1$^{-/-}$, and sham groups at day 3. Scale bar = 200 μm.

Figure 5. BB-UVB irradiation sensitizes DRG neurons through promoting the expression and function of TRPV1. (a) BB-UVB irradiation-induced changes in the expression of mRNA transcripts of Trpv1, Trpa1, Trpv3, Trpv4, Trpc4 and Trpm8 in DRG neurons. (b) Representative traces showing $[Ca^{2+}]_i$ responses evoked by 10 nM, 100 nM, 300 nM of capsaicin (3-4 independent repeats) in DRG neurons innervating the irradiated or

sham-treated skin. 100 mM KCl was used as positive control. Each colored line represents an individual cell. Statistics were shown on the right. All data were presented as mean ± SEM and analyzed with Student *t* test. *p < 0.05, **p < 0.01, ns, not significant.

Journal Pre-proof

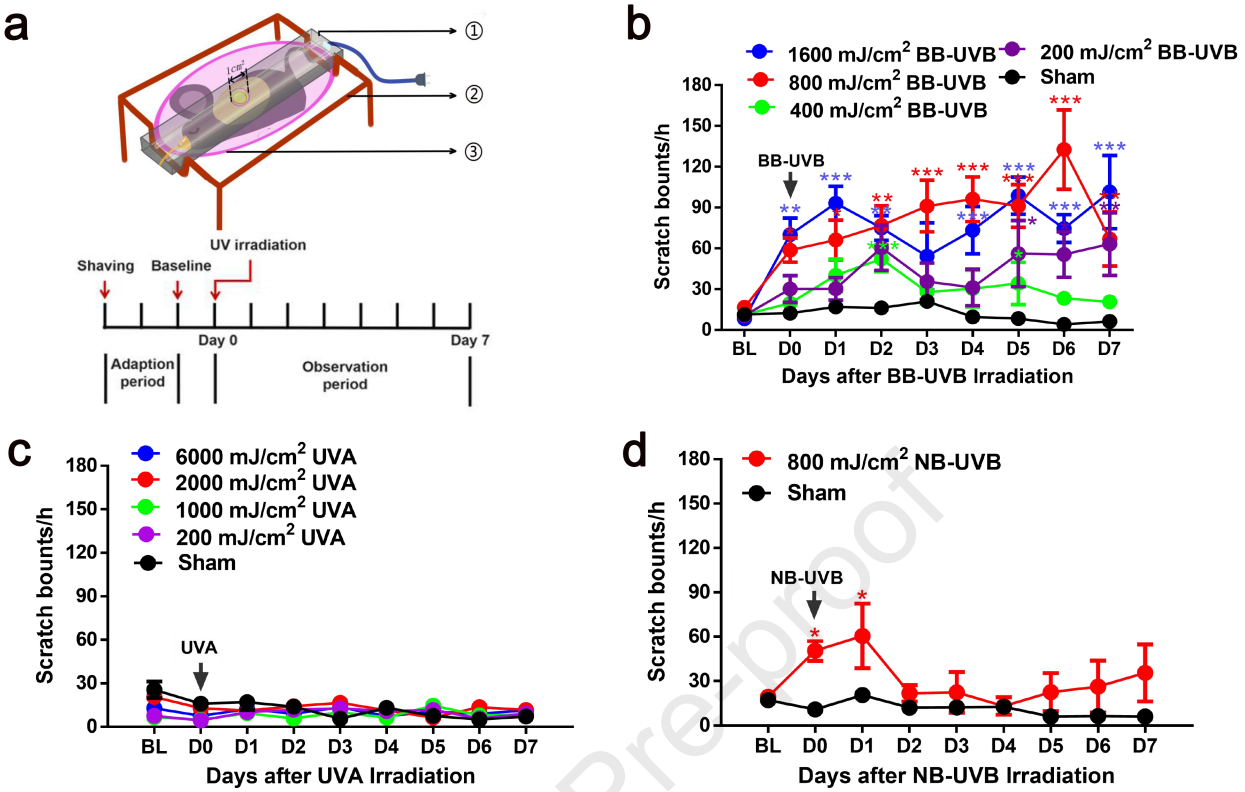

Journal Pre-proof

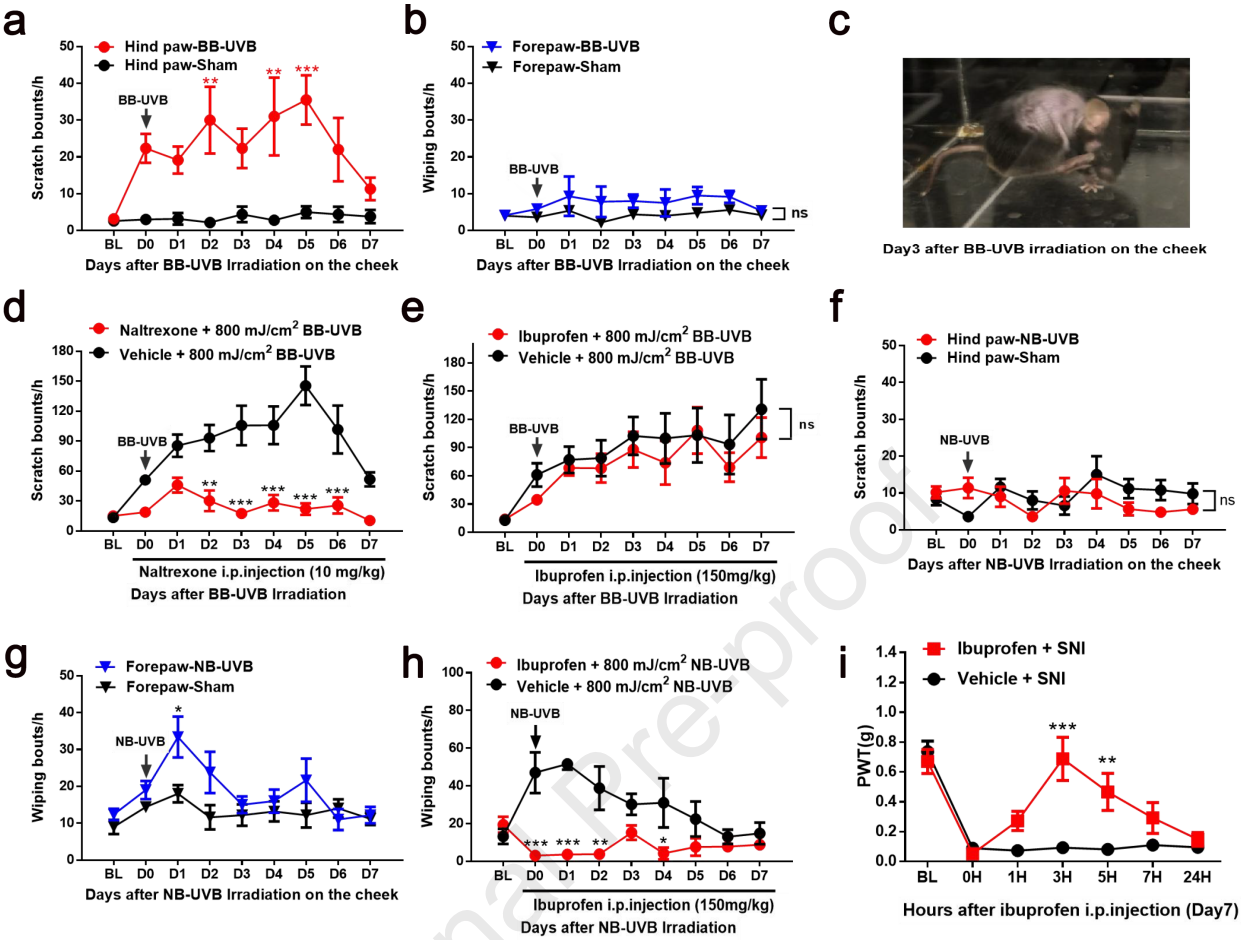

Journal Pre-proof

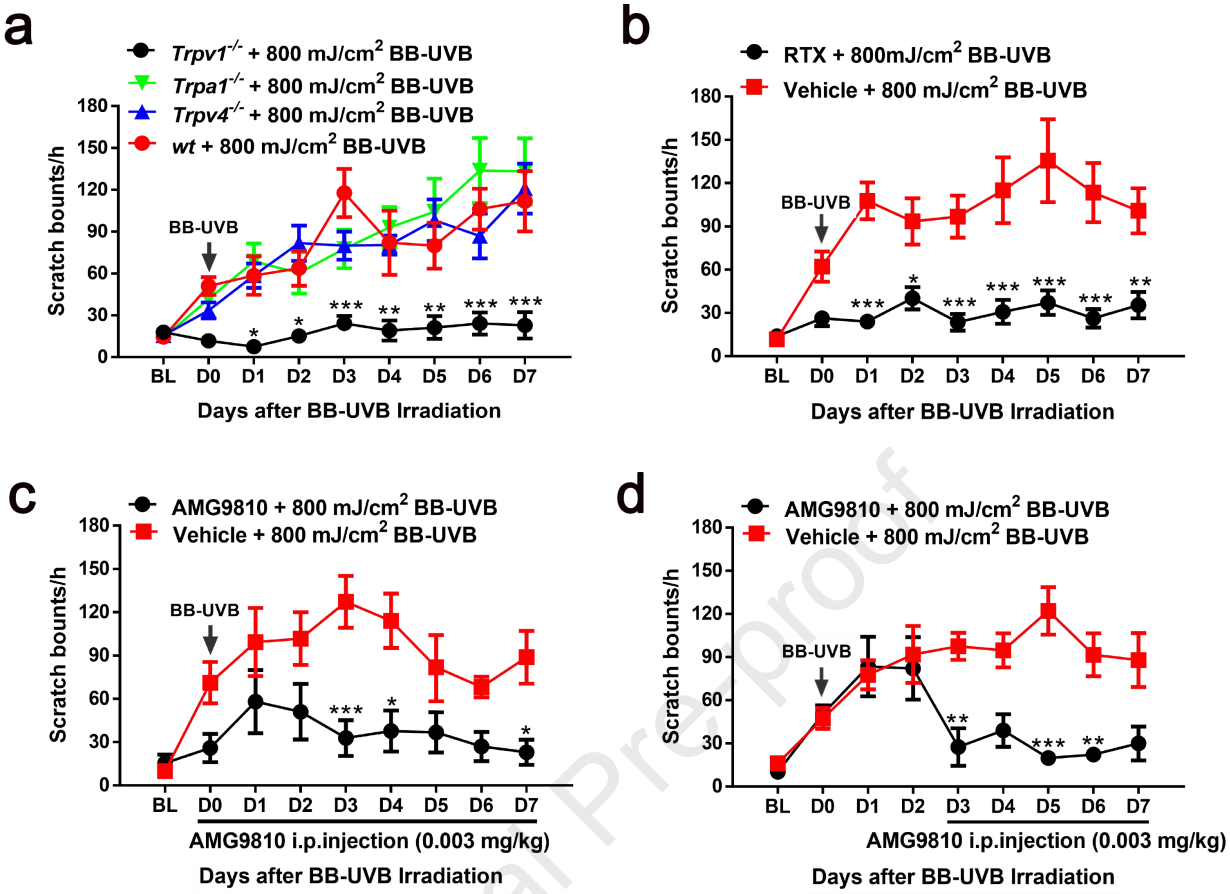

Journal Pre-proof

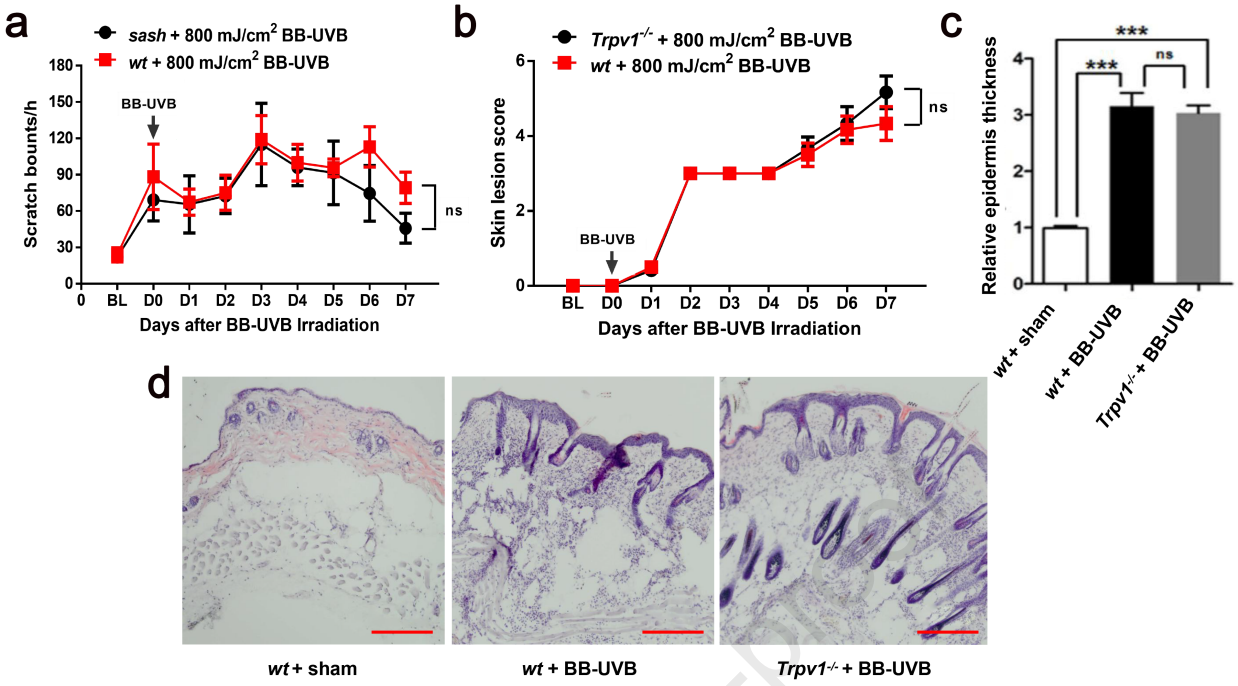

Journal Pre-proof

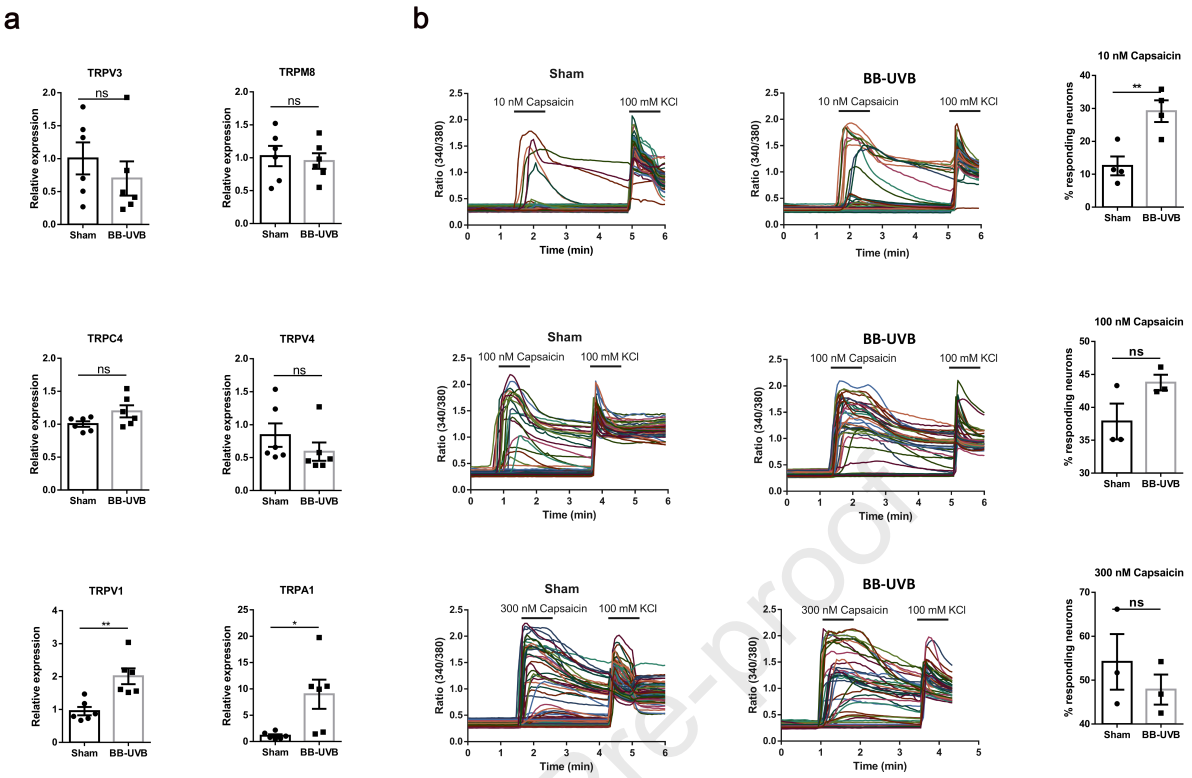

Journal Pre-proof

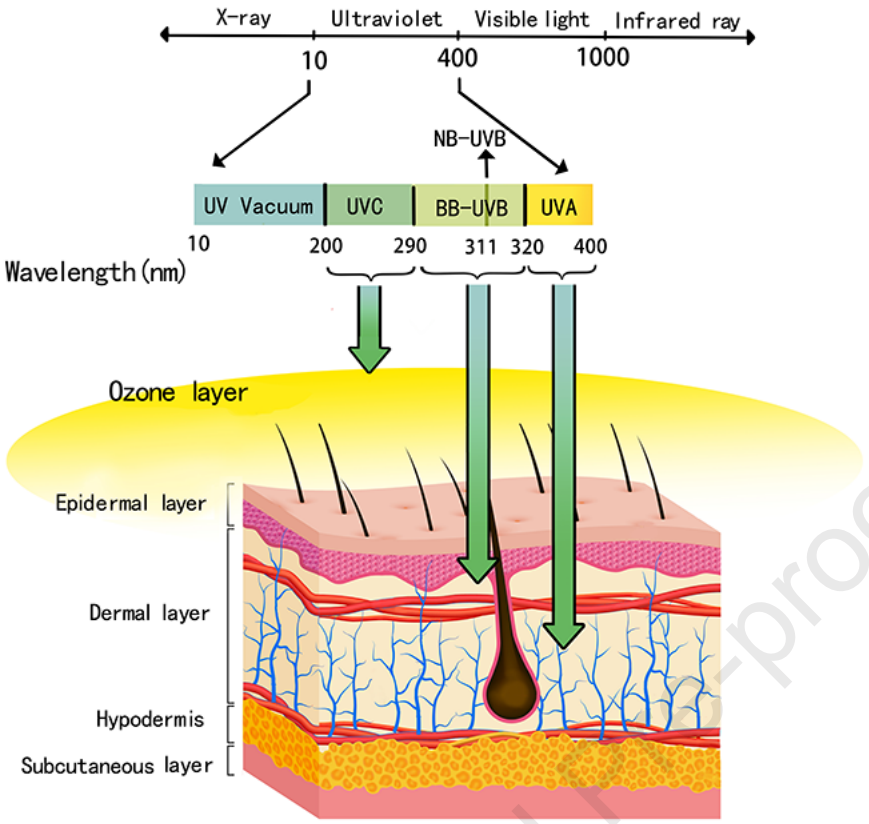

Journal Pre-proof

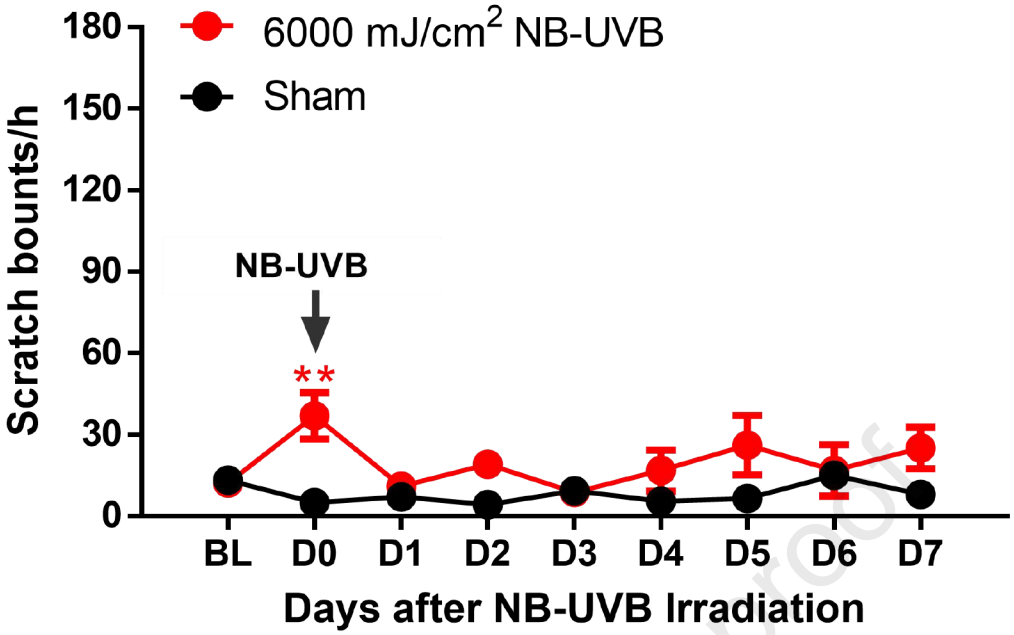

Journal Pre-proof

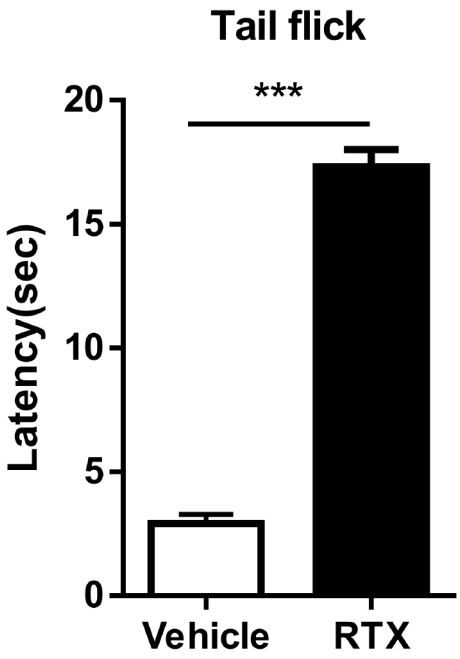

Journal Pre-proof

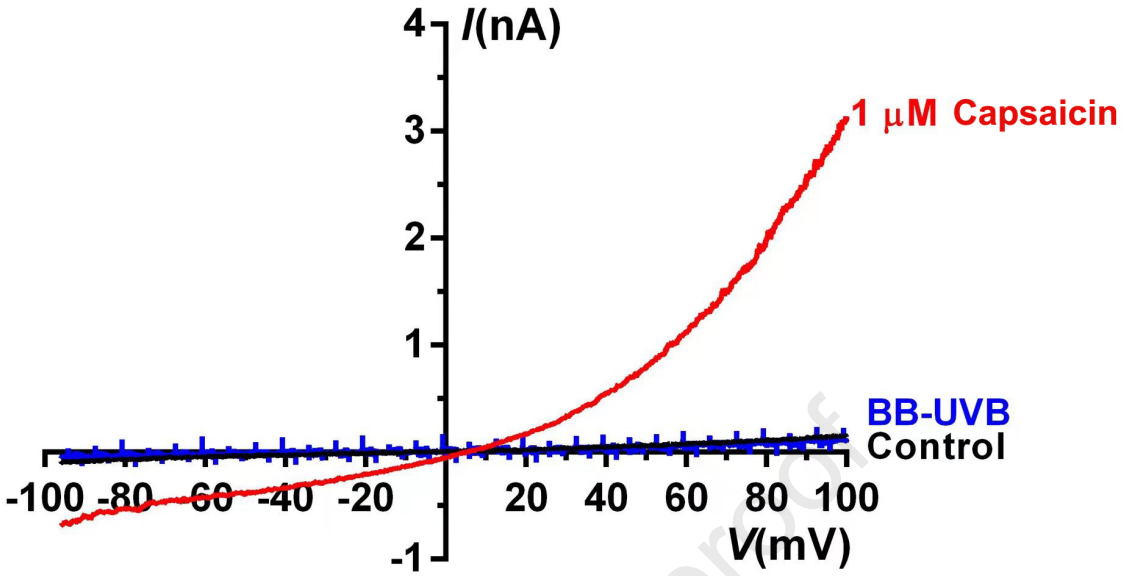

Journal Pre-proof

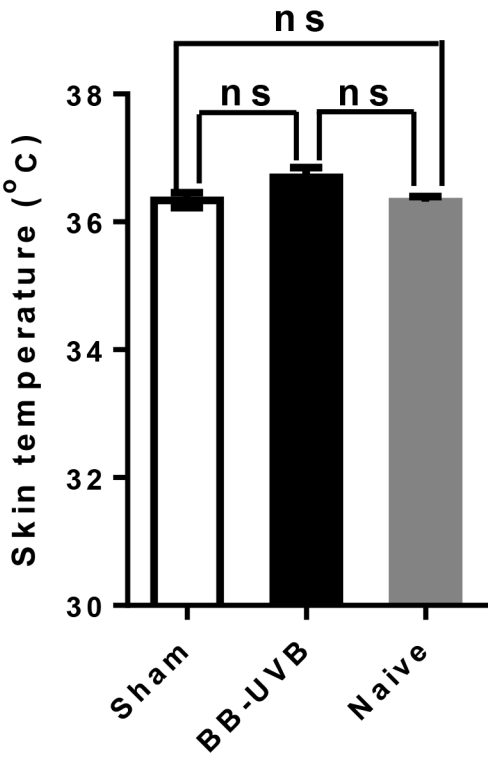

Journal Pre-proof

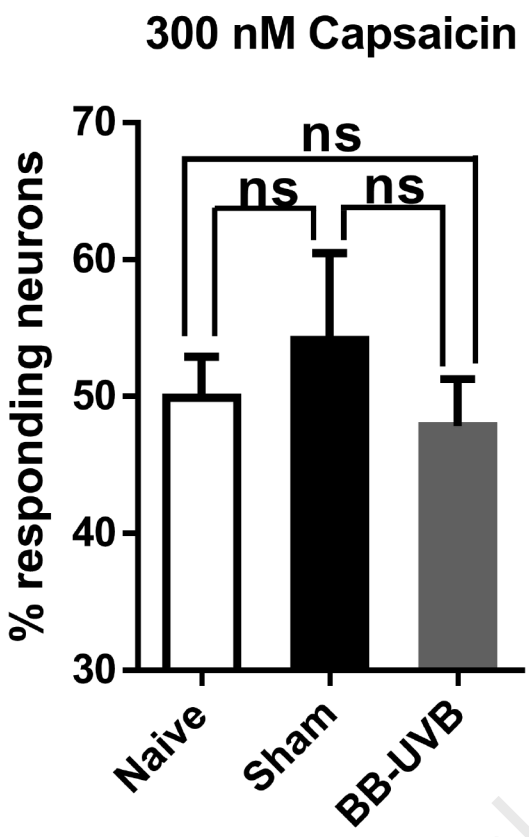

Journal Pre-proof

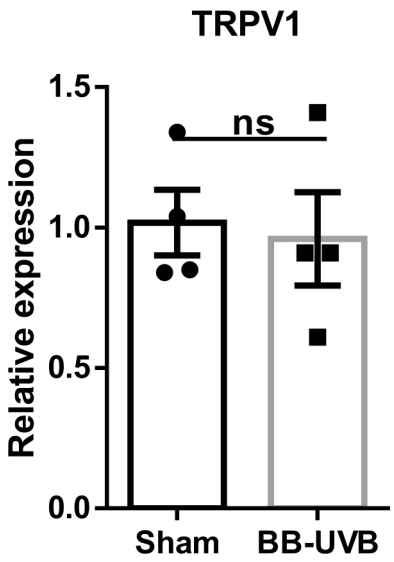

Journal Pre-proof

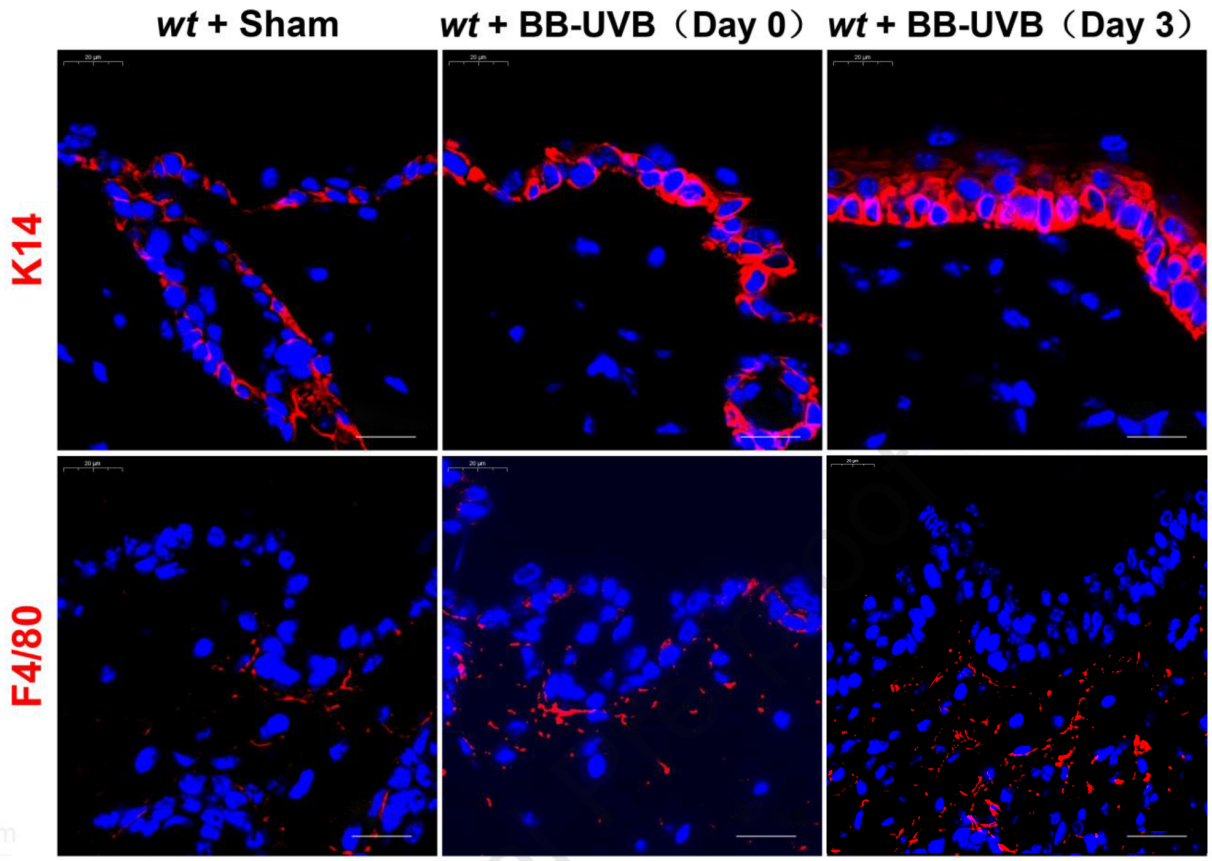

Journal

Supplementary Figure S1. Effects of UV associated with different wavelengths on skin. UV radiation in the sunlight could be divided into UVA, UVB and UVC based on the wavelength. UVA (320 to 400 nm) could penetrate into the dermal layer of the skin, UVB radiation (290 to 320 nm) is absorbed in the epidermis and superficial dermis while most of the UVC (200 to 290 nm) is absorbed by ozone layer. Specifically, NB-UVB (~311 nm) has been widely used in clinical treatment of skin disease such as psoriasis, atopic dermatitis, and vitiligo. Graph was modified from Asheesh Gupta et al. 2013 (DOI: 10.1089/wound.2012.0366).

Supplementary Figure S2. NB-UVB (6000 mJ/cm^2) induces an acute scratching response in mice. n = 6 for each group. All data were presented as mean ± SEM and analyzed with two-way ANOVA with post hoc Bonferroni test. **p < 0.01.

Supplementary Figure S3. Validation of chemical ablation of TRPV1-expressing primary afferents by RTX. n = 5 for each group. Mice treated with RTX showed a significant increment in tail flick latency when compared with mice treated with vehicle control, indicating a successful ablation of TRPV1-expressing primary afferent. All data were presented as mean ± SEM and analyzed with Student t test. ***p < 0.001.

Supplementary Figure S4. TRPV1 is not directly activated by BB-UVB irradiation. Representative TRPV1-mediated current traces induced by 1 μM capsaicin in HEK293 cells transfected with TRPV1 plasmid. BB-UVB irradiation did not activate a detectable current. Current-voltage (i-v) relations obtained from voltage-ramps from -100 to +100 mv. n= 4 independent repeats.

Supplementary Figure S5. BB-UVB irradiation does not alter skin temperature. The skin surface temperatures in sham, BB-UVB and naïve group were not significantly changed during the BB-UVB irradiation. n = 7 for each group. All data were presented as mean ± SEM and analyzed with Student t test. ns, not significant.

Supplementary Figure S6. No changes in the percentage of TRPV1-responsive DRG neurons isolated from BB-UVB-irradiated mice in response to 300 nM capsaicin. Statistics show that 300 nM of capsaicin elicited intracellular Ca^{2+} response in comparable proportions of DRG neurons innervating the irradiated skin area from naïve (n=256 cells), sham (Day3, 415 cells) or BB-UVB (Day3, n=407 cells) group from 3 independent repeats.

Supplementary Figure S7. Expression of Trpv1 mRNA transcripts in DRG neurons does not increase immediately after BB-UVB irradiation. Three mice for one dot, the total number of mice was 3×4=12 in sham and BB-UVB group. All data were presented as mean ± SEM and analyzed with Student t test. ns, not significant.

Supplementary Figure S8. Increased keratinocyte proliferation and macrophage infiltration in skin preparations from mice subjected to BB-UVB irradiation. IHC staining showed the expression patterns of K14 and F4/80 in sham and BB-UVB groups. n=3 independent repeats. Scale bar = 200 μm.

Journal Pre-proof